Limnology DOI 10.1007/s10201-008-0245-5

Computer simulations of seasonal outbreak and diurnal vertical migration of cyanobacteria

Hiroshi Serizawa, Takashi Amemiya, Axel G. Rossberg and Kiminori Itoh

H. Serizawa, T. Amemiya and K. Itoh
Graduate School of Environment and Information Sciences, Yokohama National University,
79-7 Tokiwadai, Hodogaya-ku, Yokohama 240-8501, Japan

A. G. Rossberg
Evolution and Ecology Program, International Institute for Applied Systems Analysis (IIASA),
Schlossplatz 1, 2361, Laxenburg, Austria

Abstract Algal blooms caused by cyanobacteria are characterized by two features with different time scales: one is seasonal outbreak and collapse of a bloom and the other is diurnal vertical migration. Our two-component mathematical model can simulate both phenomena, in which the state variables are nutrients and cyanobacteria. The model is a set of one-dimensional reaction-advection-diffusion equations, and temporal changes of these two variables are regulated by the following five factors: (1) annual variation of light intensity, (2) diurnal variation of light intensity, (3) annual variation of water temperature, (4) thermal stratification within a water column and (5) the buoyancy regulation mechanism. The seasonal change of cyanobacteria biomass is mainly controlled by factors, (1), (3) and (4), among which annual variations of light intensity and water temperature directly affect the maximum growth rate of cyanobacteria. The latter also contributes to formation of the thermocline during the summer season. Thermal stratification causes a reduction in vertical diffusion and largely prevents mixing of both nutrients and cyanobacteria between the epilimnion and the hypolimnion. Meanwhile, the other two factors, (2) and (5), play a significant role in diurnal vertical migration of cyanobacteria. A key mechanism of vertical migration is buoyancy regulation due to gas-vesicle synthesis and ballast formation, by which a quick reversal between floating and sinking becomes possible within a water column. The mechanism of bloom formation controlled by these five factors is integrated into the one-dimensional model consisting of two reaction-advection-diffusion equations.

Keywords ballast formation; buoyancy regulation; diurnal vertical migration; reaction-advection-diffusion equations; seasonal outbreak and collapse

Introduction

Cyanobacteria belong to the most prevalent and successful group of organisms on Earth, which have dominated various kinds of aquatic ecosystems. This group has developed some adaptive mechanisms throughout its evolutionary history, which include: phenotypic plasticity between unicellular and colonial or filamentous morphologies (Yang et al. 2006), production of toxic materials such as microcystins or anatoxins (Watanabe et al. 1996) and an ability to migrate vertically by means of buoyancy regulation (Reynolds et al. 1987). These adaptive mechanisms enable cyanobacteria to inhabit areas with extreme environmental conditions, resulting in their widespread presence in aquatic ecosystems, ranging from freshwater lakes to brackish water estuaries. In this article, we focus on the population dynamics of these organisms driven by external factors such as light intensity and water temperature, and internal factors including buoyancy regulation mechanisms.

According to Sigee (2005), the annual life cycle of colonial cyanobacteria such as *Microcystis* is as follows. These cyanobacteria overwinter as vegetative colonies on the bottom sediment until early summer. Then, some of the colonies rise into the upper water column in response to increased light intensity. Successful recruitment of benthic cells to the water column requires a preceding phase of high water clarity and light penetration to the lake bottom, which possibly cause the photo-activation of gas-vesicle synthesis. Other seasonal change that triggers the activation of dormant cells includes increasing water temperature.

The recruitment of cyanobacteria to the water column results in an algal bloom in midsummer, in which diurnal vertical migration plays an important role. For photosynthetic micro-organisms such as cyanobacteria, the primary requirement is to remain within near-surface layers where sunlight is abundant (Reynolds et al. 1987). However, photosynthetic productivity is governed not only by light but also by nutrients, which tend to be depleted in the light-rich epilimnion. Therefore, it is also advantageous for cyanobacteria to move from the nutrient-deficient epilimnion down to the metalimnion or the hypolimnion in order to take up nutrients. Buoyancy regulation of cyanobacteria is thought to have evolved to allow access to both the epilimnion and the hypolimnion (Brookes et al. 2000; Brookes and Ganf 2001; Sigee 2005).

The alternate movements within a day can be achieved by using gas-vesicles and ballast (Ibelings et al. 1991; Walsby 1994; Sigee 2005). Staying within the light-rich epilimnion promotes carbon fixation, resulting in accumulation of carbohydrates such as glycogen, which functions as ballast. As a result, cyanobacteria become heavier and begin to sink downwards when in the light. In contrast, a reduction in glycogen increases buoyancy of cyanobacteria, enabling them to return to the epilimnion for photosynthesis.

After the algal bloom in midsummer, colonial cyanobacteria fall to the bottom in autumn, where they remain viable until next early summer. This is the seasonal succession of life stages in colonial cyanobacteria. They are present in the water column over a limited period, spending most of the year in a dormant state on the lake sediments (Sigee 2005).

Theoretical studies for algal blooms seem to be classified into two different groups. The first group has focused on the seasonal change in phytoplankton population. For example, PROTECH has been presented by Reynolds et al. (2001) as a mathematical model that simulated annual population dynamics of up to eight species of phytoplankton including non-buoyant diatoms and buoyancy-regulating cyanobacteria in lakes and reservoirs. This model has succeeded in simulating both the spring diatom bloom and the summer cyanobacteria bloom as well.

Recently, Hense and Beckmann (2006) have presented a six-component model, in which the seasonal succession of cyanobacteria life stages (vegetative cells, vegetative cells with heterocysts, akinetes and recruiting cells) was simulated. Their model specifically described annual variations of the components such as nitrogen, cyanobacteria, non-migrating

phytoplankton and detritus, and typical blooms of non-migrating phytoplankton in spring and of cyanobacteria in summer were also reproduced successfully.

The second group has aimed at modeling diurnal vertical migration of cyanobacteria, focusing on buoyancy regulation mechanisms. Belov and Giles (1997) studied the growth of cyanobacteria within a calm, nutrient-saturated, isothermal water column, where some simplified conditions were imposed. For instance, light was assumed to be the only external limiting factor in their model. One unique consequence of their investigation was that cyanobacteria experienced maximum buoyancy twice a day, at dawn and at dusk. Among other attempts to model buoyancy regulation mechanisms were the studies by Visser et al. (1997), Wallace and Hamilton (2000) and Howard (2001).

These preceding studies have specifically focused on either the annual or the diurnal variation of algal population dynamics, and the comprehensive models that dealt with both phenomena have not been presented yet. Therefore, our present model is unique in respect that it can simulate both the annual and the diurnal variations of cyanobacteria. In particular, the simulation of diurnal vertical migration can be conducted successfully by introducing the ballast factor that unifies the effects of both ballast formation and reduction.

Mathematical Model

Our aim is to construct a model that describes such phenomena as diurnal vertical migration of cyanobacteria within a water column as well as the seasonal outbreak and termination of algal blooms. Nutrient concentration and cyanobacteria biomass are explicit variables of our model. Buoyancy control mechanisms are incorporated in reaction-advection-diffusion equations. To simplify the model, lateral homogeneity is assumed, meaning that two state variables are described as functions of time and depth. It is also assumed that one year consists of 365 days, and all the simulations start at midnight on December 31.

Water column

In our migration model, it is assumed that cyanobacteria that overwinter in the bottom sediments move upward to the surface in early summer and cause algal blooms in midsummer. For example, overwintering *Microcystis* colonies migrated to the epilimnion in summer in Rostherne Mere, UK, the depth of which was 30 m (Reynolds and Rogers 1976). However, Tsujimura et al. (2000) have reported that *Microcystis* colonies in the sediments at 70 and 90 m depth in the North Basin of Lake Biwa, the largest lake in Japan, did not return into the water column because gas-vesicles in the cells had collapsed due to hydrostatic pressure. They also suggested that the recruitment of *Microcystis* in the North Basin of Lake Biwa was restricted to shallow areas of less than 35 m depth (Tsujimura et al. 2000). Therefore, the depth of the water column in our model is set to be less than 30 m.

Furthermore, our model also assumes thermal stratification within the water column and the existence of a thermocline. It was reported that the thermocline existed at a depth of 6-10 m in Rostherne Mere (Sigee 2005). Synthesizing these observations, we assume that the depth of the water column z_B is 20 m and that the vertical position of the thermocline z_T is 8 m below the water surface in the present model.

Light intensity

Light intensity is one of the most important external factors regulating the behavior of the system. First, our model is constructed on the basis of periodic annual and diurnal variations of incident light intensity. If we denote incident light intensity at the surface at noon on each day by I_S, which is also the maximum value within each day, its variation follows

the formula:

$$I_S(t) = -\frac{1}{2}\left\{(I_{S\max} + I_{S\min})\cos 2\pi t + (I_{S\max} - I_{S\min})\cos\frac{2\pi(t-t_0)}{365}\right\}. \quad (1)$$

Here, I_S is a function of time t measured in days since January 1. The constants $I_{S\max}$ and $I_{S\min}$ denote maximum light intensities at the surface at noon on the day of the summer solstice and on the day of the winter solstice, respectively. The constant t_0 is the difference in time between January 1 and the winter solstice.

The vertical distribution of light intensity I at noon on each day is described as follows:

$$I(t,z) = \begin{cases} I_S(t)\exp\left(-\alpha_W z - \alpha_P \int_0^z P dz'\right) & (I_S \geq 0), \\ 0 & (I_S < 0). \end{cases} \quad (2)$$

Here, the variable z represents the depth within the water column. Light intensity is attenuated with increase in depth through absorption by water and cyanobacteria. Two constants α_W and α_P are the absorption coefficients of light by water and cyanobacteria, respectively. It is assumed that light attenuation by other phytoplankton is constant and encompassed within the α_W term. The annual variation of light intensity at the surface is shown in Fig. 1 (a).

Water temperature

Water temperature is another external factor that controls the growth rate of cyanobacteria (Bowie et al. 1985). Another basis of our model is the periodic annual variation of water temperature at the surface. However, the seasonal variation of temperature within a water column also depends on depth. For example, water temperature varied between about 5°C and 20°C at the surface, while it varied between about 5°C and 10°C at 20 m depth in Rostherne Mere (Reynolds and Rogers 1976).

The vertical distribution of water temperature, in any lake, is influenced by such physical factors as surface wind and water movement. In particular, a steep thermal gradient, the thermocline, is created due to the combined effect of heating near the surface and stagnation of water movement near the bottom during the summer season (Reynolds et al. 2001). A marked thermocline largely prevents vertical mixing and significantly affects the vertical distribution of both phytoplankton and nutrients within the water column. During the winter season, in monomictic lakes such as Rostherne Mere, water temperature is almost uniform, resulting in complete mixing of the whole lake (Reynolds and Rogers 1976).

In the present work, we schematically assume that water temperatures both at the surface and at the bottom vary annually, while the amplitude of the variation at the surface is larger than that at the bottom. Water temperature at the surface is lowest and the same as that at the bottom on January 31, which is the coldest day of the year in our model. Annual variations of water temperature at the surface and at the bottom are shown in Fig. 1 (a). The values of water temperature are arbitrary.

Maximum growth rate of cyanobacteria

The relationship between the maximum growth rate μ_m and water temperature T follows the formula:

$$\mu_m(T) = \mu_m(T_0)\exp\{\beta(T - T_0)\}. \quad (3)$$

Here, T_0 denotes the reference temperature and β is the constant (Bowie et al. 1985; Reynolds et al. 2001).

In this article, the annual variation of water temperature shown in Fig. 1 (a) is a rough approximation and its mathematical representation is not specified. Therefore, we use the following formulae for annual variations of the maximum growth rates of cyanobacteria at the water surface μ_{mS} and at the bottom μ_{mB} as a function of time t.

$$\mu_{mS}(t) = \frac{1}{2}\left\{(\mu_{mS\max} + \mu_{mS\min}) - (\mu_{mS\max} - \mu_{mS\min})\cos\frac{2\pi(t-t_1)}{365}\right\}, \tag{4}$$

$$\mu_{mB}(t) = \frac{1}{2}\left\{(\mu_{mB\max} + \mu_{mS\min}) - (\mu_{mB\max} - \mu_{mB\min})\cos\frac{2\pi(t-t_1)}{365}\right\}. \tag{5}$$

Four constants $\mu_{mS\max}$, $\mu_{mS\min}$, $\mu_{mB\max}$ and $\mu_{mB\min}$ respectively denote the maximum growth rate of cyanobacteria at the surface and at the bottom on the warmest day and on the coldest day. Our model assumes that $\mu_{mS\min}=\mu_{mB\min}$, which means that the maximum growth rate is constant throughout the water column on the coldest day, January 31. One more constant t_1 is the difference between January 1 and the coldest day. Figure 1 (b) shows annual variations of the maximum growth rate at the surface μ_{mS} and at the bottom μ_{mB}.

Next, we consider the dependence of the maximum growth rate on depth z. We must take into account the stratification of water temperature and the existence of the thermocline within the intermediate region of the water column during summer. Denoting the vertical extent and the depth of the thermocline as w_T and z_T, we can formulate the maximum growth rate μ_m, as follows:

$$\mu_m(t,z) = \mu_{mB}(t) + \{\mu_{mS}(t) - \mu_{mB}(t)\}\frac{1}{2}\left(1 - \frac{z - z_T}{\sqrt{{w_T}^2 + (z - z_T)^2}}\right). \tag{6}$$

Vertical profiles of the maximum growth rate are shown in Fig. 1 (c) for January 1, April 1, July 1 and October 1, representing four seasons. As stated previously, the depth of the water column is z_B=20 m and the depth of the thermocline is z_T=8 m in our model.

Actual growth rate

The actual growth rate μ is described by a product of the maximum growth rate μ_m and the minimum function f, as follows (Yoshiyama and Nakajima 2002; Huisman et al. 2006):

$$f(I(t,z), N(t,z)) = \min\left(\frac{I(t,z)}{I(t,z) + H_I}, \frac{N(t,z)}{N(t,z) + H_N}\right). \tag{7}$$

$$\mu(t,z) = \mu_m(t,z) f(I(t,z), N(t,z)). \tag{8}$$

The minimum function f gives the smaller value of two Monod functions for light intensity I and nutrient concentration N. Two parameters H_I and H_N are half-saturation constants for I and N, respectively.

The actual growth rate is restricted by the smaller value of two Monod functions for I and N. Therefore, either light intensity or nutrient concentration determines the actual growth rate at each time. At night, the actual growth rate falls to zero due to the absence of light.

Turbulent diffusivity

The thermocline not only affects the vertical distribution of the maximum growth rate of cyanobacteria, but also largely prevents vertical diffusive mixing within the water column. The turbulent diffusivity D depends on depth z, reflecting mixing by surface processes. The turbulent diffusivity at the bottom D_B is a function of time t, which is represented as follows:

$$D_B(t) = \frac{1}{2}\left\{(D_{B\max} + D_{B\min}) + (D_{B\max} - D_{B\min})\cos\frac{2\pi(t-t_1)}{365}\right\}. \tag{9}$$

According to the equation (9), D_B shows the maximum on January 31, with the value denoted as $D_{B\max}$, while the

minimum turbulent diffusivity at the bottom $D_{B\min}$ occurs on the warmest day in midsummer. Annual variations of turbulent diffusivities at the surface D_S and at the bottom D_B are shown in Fig. 1 (b). The value of D_S is set as constant throughout the year.

As a result, the depth dependence of the turbulent diffusivity D follows the representation:

$$D(t,z) = D_B(t) + (D_S - D_B(t))\frac{1}{2}\left(1 - \frac{z - z_T}{\sqrt{{w_T}^2 + (z - z_T)^2}}\right). \tag{10}$$

Vertical profiles of the turbulent diffusivity are also shown in Fig. 1 (c) for January 1, April 1, July 1 and October 1.

Buoyancy regulation mechanism

If we denote the vertical velocity and the cell density of cyanobacteria by V and ρ_P, we can derive the following relationship between V and ρ_P from Stokes' law by comparing the densities of cyanobacteria ρ_P and water ρ_W (Reynolds et al. 1987; Visser et al. 1997; Wallace and Hamilton 2000).

$$V(t,z) \propto \rho_P(t,z) - \rho_W. \tag{11}$$

Differentiating this formula (11) with respect to time leads to the following relationship:

$$\frac{\partial}{\partial t}V(t,z) \propto \frac{\partial}{\partial t}\rho_P(t,z) \propto \mu(t,z). \tag{12}$$

We assume that the differential of the cell density is proportional to the actual growth rate μ. This assumption is based on the results of preceding studies which showed that the rate of increase in cell density was a Monod function of light intensity in nutrient-saturated, isothermal conditions (Kromkamp and Walsby 1990; Visser et al. 1997; Wallace and Hamilton 2000). Although the condition of our model is neither nutrient-saturated nor isothermal, the formula (12) could be a natural extension, because the actual growth rate μ is represented by the equations (7) and (8).

Ballast factor

Buoyancy of cyanobacteria is controlled by carbohydrate accumulation and ballast formation, which affects the cell density ρ_P. Here, we define the ballast factor F, which is a function of time t and depth z, as an integration of the actual growth rate μ, as follows:

$$F(t,z) = \int_0^\infty \mu(t-\tau,z)e^{-k\tau}d\tau = \int_0^\infty \mu_m(t-\tau,z)[f(I(t-\tau,z),N(t-\tau,z))]e^{-k\tau}d\tau. \tag{13}$$

We assume that the ballast factor F is determined by previous light and nutrient histories and that the contribution of the past growth rate decays exponentially in the progress of time. Therefore, the overall contribution of previous histories is represented by integration of the product of the actual growth rate μ and an exponential decay factor $\exp(-k\tau)$, where k is the reciprocal of decay time and τ is the variable for integration.

Finally, the following representation describes vertical movement of cyanobacteria:

$$V(t,z) = V_m \times \{F(t,z) - F_0\}. \tag{14}$$

The constant V_m is the scale factor for the velocity of vertical migration and the parameter F_0 represents the ballast factor for neutral buoyancy, i.e., the equilibrium between floating and sinking, which is a key parameter in our model. In the case of $F=F_0$, cyanobacteria are suspended within the water column. A ballast factor smaller than F_0 ($F<F_0$) induces floating, while that larger than F_0 ($F>F_0$) results in sinking.

Reaction-advection-diffusion equations

The spatio-temporal dynamics of nutrient concentration and cyanobacteria biomass is described by the following partial differential equations (Yoshiyama and Nakajima 2002; Fennel and Boss 2003; Huisman et al. 2006):

$$\frac{\partial N}{\partial t} = \frac{\partial}{\partial z}\left(D\frac{\partial N}{\partial z} \right) - a\mu P + \varepsilon a m_P P, \tag{15}$$

$$\frac{\partial P}{\partial t} = \frac{\partial}{\partial z}\left(D\frac{\partial P}{\partial z} \right) - \frac{\partial}{\partial z}(VP) + \mu P - m_P P. \tag{16}$$

Two dependent variables N and P represent nutrient concentration and cyanobacteria biomass. Time and depth-dependent D and V specify the vertical turbulent diffusivity and the vertical velocity of cyanobacteria, respectively. m_P is the mortality rate of cyanobacteria, a is the nutrient content in cyanobacteria and ε is the recycled proportion of the nutrients in dead cyanobacteria.

Since the value of μ changes periodically with time, this is a forced oscillatory system. The peculiarity of the system is that it oscillates at two different frequencies, i.e., yearly and daily, due to annual and diurnal variations of light intensity and water temperature.

Parameters

The definitions and values of parameters are listed in Table 1. Most of the parameter values are chosen from preceding studies (Bowie et al. 1985; Reynolds et al. 1987; Brookes and Ganf 2001; Long et al. 2001; Yoshiyama and Nakajima 2002; Huisman et al. 2004; Sigee 2005; Huisman et al. 2006), while some are assigned during this work.

Herewith are some comments on the choice of parameter values. The coefficient of absorption by 1 g of cyanobacteria α_P is calculated by the division $\alpha_{P\text{cell}}/m_{\text{cell}}$, where $\alpha_{P\text{cell}}$ and m_{cell} denote the absorption coefficient by a cyanobacterium cell and the dry weight of a cell, respectively. The nutrient content in 1 g of cyanobacteria a is also estimated by the division $a_{\text{cell}}/m_{\text{cell}}$, where a_{cell} denotes the nutrient content in a cyanobacterium cell. As for the reciprocal of decay time for the actual growth rate k and the scale factor for the velocity of cyanobacteria V_m, we discuss these below.

Boundary conditions and initial conditions

We assume the following boundary conditions at the surface (z=0) and at the bottom (z=z_B) of the water column.

$$\frac{\partial N}{\partial z} = 0, \quad \frac{\partial P}{\partial z} = \frac{V_m}{D(t,0)}\{(F(t,0) - F_0\}P \quad (z = 0). \tag{17}$$

$$N = N_B, \quad \frac{\partial P}{\partial z} = 0 \qquad\qquad (z = z_B). \tag{18}$$

Here, N_B denotes the nutrient concentration at the bottom, which does not vary throughout the year. This means that nutrients are continuously supplied from the bottom. Otherwise, the usual zero-flux boundary conditions are imposed.

Computer simulations are carried out under the following conditions. The one-dimensional water column is divided into 100 layers. Therefore, the thickness of each layer is 0.2 m. The fourth order Runge-Kutta integrating method is applied with a time step Δt=0.005 day. It is confirmed that the results with smaller time steps remain the same for each program, ensuring the accuracy of the simulations.

Results

The model gradually settles into yearly periodic oscillations with superimposed daily oscillations, independent of initial

conditions. The results shown here are those during the second year after the one-year start up. It is confirmed that the system shows repetitive oscillations after the first year.

Annual variation of cyanobacteria biomass

Figure 2 shows annual variations of nutrient concentration (broken line) and cyanobacteria biomass (solid line), using diurnally averaged values. The values of both components are also spatially averaged within the layers between 0 and 2 m depth. A sudden increase in cyanobacteria biomass P occurs during June, showing a peak at the beginning of July. The maximum value of P at the peak is more than 5.6 g/m^3. The value of P begins to reduce in July, and a gradual decrease continues until the end of the year.

Meanwhile, nutrient concentration N begins to decrease during June because of uptake by cyanobacteria. The value of N shows a minimum in August, with a gradual recovery of concentration continuing until the beginning of the next year.

The annual variation of the depth profile of cyanobacteria biomass P is shown in Fig. 3. The values of P are diurnally averaged. Mass occurrence of cyanobacteria during a few months between June and August is obviously observed above the thermocline, particularly in the layers between 0 and 5 m. In contrast, cyanobacteria are at low levels in the layers below the thermocline throughout the year.

Referring to the observations by Takamura and Yasuno (1984) in hypertrophic Lake Kasumigaura, Japan, we define an algal bloom as the state in which the amount of cyanobacteria biomass accumulated at the surface exceeds 1.0×10^5 cells/ml, i.e., 1.0×10^{11} cells/m^3. This value corresponds to 4.0 g/m^3, considering that the dry weight of a cyanobacterium cell m_{cell} is 40.0×10^{-12} g/cell (Table 1). Judging from the value of P in Fig. 2, we can claim that the algal bloom occurs during about one and a half months from the middle of June to the beginning of August.

Diurnal variation of cyanobacteria biomass

Figure 4 shows diurnal variations of light intensity at the surface I_S (broken lines) and cyanobacteria biomass P of different layers (solid lines). The period is from noon July 10 to noon July 11, in the midst of the algal bloom. Four solid lines labeled 0, 1, 2 and 3 show cyanobacteria biomass averaged within the layers between 0 and 2 m, 2 and 4 m, 4 and 6 m, and 6 and 8 m below the surface, respectively. The movement of the peak in the order of lines labeled 3, 2, 1 and 0 corresponds to the ascent of cyanobacteria.

The diurnal variation of the depth profile of cyanobacteria biomass P is shown in Fig. 5. The period is from noon July 10 to noon July 11, which is the same period as in Fig. 4. The cyanobacteria peak concentrations provide evidence of descent and ascent, corresponding to vertical migration.

Figure 6 shows a comparison between field data (●) and the computer simulation (solid line) for diurnal variation of cyanobacteria biomass in near-surface layers between 0 and 1 m. The field data were taken in Lake Vinkeveen, the Netherlands, in late August (Ibelings et al. 1991). It seems that the simulation resulting from our model shows similar tendencies to the field data. For example, the maximum of cyanobacteria biomass in the early morning reproduced in our model shows an approximate agreement with the field observation.

Diurnal variation of ballast factor

Figure 7 shows the diurnal variation of the ballast factor F (solid lines) from noon July 10 to noon July 11 in the layers between 0 and 4 m (line 0), 4 and 8 m (line 1), and 8 and 20 m (line 2) depth, respectively. The two lines labeled 0 and 1 show the variation of F above the thermocline, while the line labeled 2 shows that below the thermocline. The ballast

factor for neutral buoyancy F_0=0.1 is also indicated (broken line).

Discussion

Comparison with field observations for annual variation

A number of surveys have been conducted of the seasonal variation of bloom-forming cyanobacteria in natural lakes (Hanazato et al. 1991; Tsujimura et al. 2000). The observations that algal blooms broke out in early summer and collapsed in autumn have been commonly reported all over the world (Reynolds and Rogers 1976). Our simulations follow these observations, as shown in Figs 2 and 3.

The seasonal drop in nutrient concentration that started with the onset of the algal bloom season has also been reported (Wakabayashi and Ichise 2004; Sigee 2005). The decrease in nutrient concentration from uptake by cyanobacteria during summer is also simulated in our model, as shown in Fig. 2.

Comparison with field observations for diurnal variation

According to Sigee (2005), the general view of diurnal vertical migration of cyanobacteria is as follows. During daytime, high rates of ballast formation by photosynthesis at the lake surface result in decreased buoyancy, causing sinking of cyanobacteria within the water column. The reverse process, i.e., cyanobacteria rising up the water column, occurs at night. These movements and the consequent diurnal oscillation of cyanobacteria biomass in the surface layers have been confirmed by Takamura and Yasuno (1984), Ibelings et al. (1991), Visser et al. (1996), Ha et al. (2000) and others. Our simulations show such a diurnal periodic oscillation, as seen in Figs 4 and 5.

Alternation of floating and sinking above the thermocline

The ballast factor F is defined as an integration of the actual growth rate. Comparing the vertical distribution of F with F_0 in Fig. 7, we find that sinking is dominant from the late morning to the evening in near-surface layers above 4 m depth, whereas floating is dominant from midnight to the early morning (line 0). In other regions below 4 m depth, floating is dominant throughout the day (lines 1 and 2). We also point out that the positive plateau of the ballast factor F in near-surface layers during the afternoon (line 0) can explain field observations by Visser et al. (1996), which showed buoyancy loss in *Microcystis* colonies, i.e., the increase in colonies sinking, during the day in the shallow part of De Gijster reservoir, the Netherlands.

As mentioned before, the ballast factor for neutral buoyancy F_0 is a key parameter that regulates cyanobacteria distributions. In the present study, we adopt the value of F_0=0.1, though the value of F_0 should be derived from Stokes' law referring to the density of water ρ_W. The choice of the parameter value can be justified for the following reasons. As shown in Fig. 7, the highest value of the ballast factor F is about 0.14 in near-surface layers (line 0), while the lowest value is almost 0 in deep layers below the thermocline (line 2). Therefore, the value of F_0 should be within this range (0-0.14) in order that both floating and sinking can take place within the water column. When F_0=0.1 as in the present study, the value of the difference between F and F_0 ranges from about -0.1 to 0.04. If we consider that the scale factor is V_m=250 m/day, the values of the vertical velocity of cyanobacteria range from -25 m/day (floating) to 10 m/day (sinking). These values show a good agreement with the vertical velocity of *Microcystis* estimated at -30 m/day to 10 m/day by Reynolds et al. (1987).

We admit that similar vertical movements are observed within a certain range of F_0, at least $0.08 \leq F_0 \leq 0.12$. However, in the case of F_0=0, no algal bloom occurs, because cyanobacteria always sink down to the bottom in such a condition.

Further attention should be paid to the parameter k, which denotes the reciprocal of the decay time for the contribution of the actual growth rate to ballast formation. Our model adopts k=3, meaning that the contribution of the actual growth rate reduces to 1/e in 8 hours. It should be noted that this value is comparable with the lifetime of ballast, which was estimated by Reynolds et al. (1987) to be 4 to 12 hours.

Comparison with other models

The population dynamics of cyanobacteria are characterized by such phenomena as seasonal outbreak and sudden disappearance, and diurnal vertical migration, which develop on different time scales. The most striking feature of our model is that it can simulate both phenomena as well.

Until now, a number of mathematical models have been presented to explain some aspects of cyanobacterial population dynamics. Both PROTECH by Reynolds et al. (2001) and a six-component model by Hense and Beckmann (2006) have succeeded in simulating the annual variation including a summer bloom. However, these models specifically described seasonal changes, and diurnal changes were excluded.

As for the diurnal change, on the other hand, the model by Belov and Giles (1997) focused on population dynamics within a calm, nutrient-saturated, isothermal water column. Therefore, the phenomena such as turbulent mixing and thermal stratification were not considered in their model, which seemed to be of great importance in simulating the annual and the diurnal variations of cyanobacteria.

Our mathematical model presents comprehensive explanations for both the annual and the diurnal population dynamics of cyanobacteria. In particular, the buoyancy regulation mechanism, i.e., diurnal periodic alternation between floating and sinking in the upper layers is successfully simulated by introducing the ballast factor. It should be noted that our model includes the effects of turbulent mixing and thermal stratification, which were neglected by Belov and Giles (1997).

Acknowledgments We are grateful to T. Enomoto and K. Shibata for insightful discussions. This study is supported by the Global COE Program "Global Eco-Risk Management from Asian View Points" from the Ministry of Education, Culture, Sports, Science and Technology of Japan.

References

Belov AP, Giles JD (1997) Dynamical model of buoyant cyanobacteria. Hydrobiologia 349:87-97

Bowie GL, Mills WB, Porcella DB, Campbell CL, Pagenkopf JR, Rupp GL, Johnson KM, Chan PWH, Gherini SA (1985) Rates, constants, and kinetics formulations in surface water quality modeling. U.S. Environmental Protection Agency, Athens, Georgia, U.S.A.

Brookes JD, Ganf GG, Oliver RL (2000) Heterogeneity of cyanobacterial gas-vesicle volume and metabolic activity. J Plankton Res 22:1579-1589

Brookes JD, Ganf GG (2001) Variations in the buoyancy response of *Microcystis aeruginosa* to nitrogen, phosphorus and light. J Plankton Res 23:1399-1411

Fennel K, Boss E (2003) Subsurface maxima of phytoplankton and chlorophyll: steady-state solutions from a simple model. Limnol Oceanogr 48:1521-1534

Ha K, Kim H-W, Jeong K-S, Joo G-J (2000) Vertical distribution of *Microcystis* population in the regulated Nakdong River, Korea. Limnology 1:225-230

Hanazato T, Aizaki M (1991) Changes in species composition of cladoceran community in Lake Kasumigaura during 1988-1989: occurrence of *Daphnia galeata* and its effect on algal biomass. Jpn J Limnol 52:45-55

Hense I, Beckmann A (2006) Towards a model of cyanobacteria life cycle—effects of growing and resting stages on bloom formation of N_2–fixing species. Ecol Model 195:205-218

Howard A (2001) Modeling movement patterns of the cyanobacterium, *Microcystis*. Ecol Appl 11:304-310

Huisman J, Sharples J, Stroom JM, Visser PM, Edwin W, Kardinaal A, Jolanda M, Verspagen H, Sommeijer B (2004) Changes in turbulent mixing shift competition for light between phytoplankton species. Ecology 85:2960-2970

Huisman J, Thi NNP, Karl DM, Sommeijer B (2006) Reduced mixing generates oscillations and chaos in the oceanic deep chlorophyll maximum. Nature 439:322-325

Ibelings BW, Mur LR, Walsby AE (1991) Diurnal changes in buoyancy and vertical distribution in populations of *Microcystis* in two shallow lakes. J Plankton Res 13:419-436

Kromkamp J, Walsby AE (1990) A computer model of buoyancy and vertical migration in cyanobacteria. J Plankton Res 12:161-183

Long BM, Jones GJ, Orr PT (2001) Cellular microcystin content in N-limited *Microcystis aeruginosa* can be predicted from growth rate. Appl Environ Microbiol 67:278-283

Reynolds CS, Rogers DA (1976) Seasonal variations in the vertical distribution and buoyancy of *Microcystis aeruginosa* Kütz. Emend. Elenkin in Rostherne Mere, England. Hydrobiologia 48:17-23

Reynolds CS, Oliver RL, Walsby AE (1987) Cyanobacterial dominance: the role of buoyancy regulation in dynamic lake environments. NZ J Mar Freshwater Res 21:379-390

Reynolds CS, Irish AE, Elliott JA (2001) The ecological basis for simulating phytoplankton responses to environmental change (PROTECH). Ecol Model 140:271-291

Sigee DC (2005) Freshwater Microbiology. John Wiley and Sons Ltd, West Sussex, England.

Takamura N, Yasuno M (1984) Diurnal changes in the vertical distribution of phytoplankton in hypertrophic Lake Kasumigaura, Japan. Hydrobiologia 112:53-60

Tsujimura S, Tsukada H, Nakahara H, Nakajima T, Nishino M (2000) Seasonal variations of *Microcystis* populations in sediments of Lake Biwa, Japan. Hydrobiologia 434:183-192

Visser PM, Ketelaars HAM, van Breemen LWCA, Mur LR (1996) Diurnal buoyancy changes of *Microcystis* in an artificially mixed storage reservoir. Hydrobiologia 331:131-141

Visser PM, Passarge J, Mur LR (1997) Modelling vertical migration of the cyanobacterium *Microcystis*. Hydrobiologia 349:99-109

Wakabayashi T, Ichise S (2004) Seasonal variation of phototrophic picoplankton in Lake Biwa (1994-1998). Hydrobiologia 528:1-16

Wallace BB, Hamilton DP (2000) Simulation of water-bloom formation in the cyanobacterium *Microcystis aeruginosa*. J Plankton Res 22:1127-1138

Walsby AE (1994) Gas vesicles. Microbiol Rev 58:94-144

Watanabe MF, Harada K, Carmichael WW, Fujiki H (1996) Toxic *Microcystis*. CRC Press Inc, Boca Raton, Florida, U.S.A.

Yang Z, Kong F, Shi X, Cao H (2006) Morphological response of *Microcystis aeruginosa* to grazing by different sorts of

zooplankton. Hydrobiologia 563:225-230

Yoshiyama K, Nakajima H (2002) Catastrophic transition in vertical distributions of phytoplankton: alternative equilibria in a water column. J Theor Biol 216:397-408

Table 1. Parameters in the mathematical model.

Parameters	Meanings	Values	Units	Values in references
$I_{S\max}$	Maximum light intensity at the surface at noon on the summer solstice	800	$\mu mol \cdot m^{-2} \cdot s^{-1}$	600[e)]
$I_{S\min}$	Maximum light intensity at the surface at noon on the winter solstice	400		
d_0	Difference between Jan. 1 and the winter solstice	-10	day	i)
α_W	Absorption coefficient by water	0.23	m^{-1}	0.2[e)]
$\alpha_{P\text{cell}}$	Absorption coefficient by cyanobacteria	2.4×10^{-12}	m^2/cell	3.4×10^{-12} [f)]
m_{cell}	Dry weight of cyanobacteria	40.0×10^{-12}	g/cell	$17.7\text{-}43.4\times10^{-12}$ [d)]
α_P	Absorption coefficient by cyanobacteria	0.06	m^2/g	$=\alpha_{P\text{cell}}/m_{\text{cell}}$
$\mu_{mS\max}$	Maximum growth rate of cyanobacteria at the surface on the warmest day	0.58	day^{-1}	0.21-0.75[c)] 1.0[e)], 0.48[g)]
$\mu_{mS\min}$	Maximum growth rate of cyanobacteria at the surface on the coldest day, Jan. 31	0.1		
$\mu_{mB\max}$	Maximum growth rate of cyanobacteria at the bottom on the warmest day	0.2		
$\mu_{mB\min}$	Maximum growth rate of cyanobacteria at the bottom on the coldest day, Jan. 31	0.1		
d_1	Difference between Jan. 1 and the coldest day	30	day	i)
H_I	Half-saturation constant for light intensity	20.0	$\mu mol \cdot m^{-2} \cdot s^{-1}$	20.0[e)]
H_N	Half-saturation constant for nutrient concentration	0.2	$mmol/m^3$	0.2[e)]
D_S	Vertical turbulent diffusivity at the surface	5.0	m^2/day	4.32[e)]
$D_{B\max}$	Vertical turbulent diffusivity at the bottom on the coldest day, Jan. 31	5.0		
$D_{B\min}$	Vertical turbulent diffusivity at the bottom on the warmest day	1.0		
k	Reciprocal of decay time for actual growth rate	3.0	day^{-1}	comparable to b)
V_m	Scale factor for velocity of cyanobacteria	250.0	m/day	comparable to b)
F_0	Ballast factor for neutral buoyancy	0.1		i)
a_{cell}	Nutrient content in cyanobacteria	0.6×10^{-10}	mmol/cell	$0.52\text{-}4.38\times10^{-10}$ [a)]
a	Nutrient content in cyanobacteria	1.5	mmol/g	$=a_{\text{cell}}/m_{\text{cell}}$
ε	Recycling rate of nutrient in dead cyanobacteria	0.5		0.5[h)]
m_P	Mortality rate of cyanobacteria	0.15	day^{-1}	0.2[e)]
N_B	Nutrient concentration at the bottom	40	$mmol/m^3$	40[e)]
w_T	Vertical extent of the thermocline	1	m	i)
z_T	Depth of the thermocline	8	m	18[e)]
z_B	Depth of the water column	20	m	50[e)], 18[f)]

The simulations by the mathematical model are carried out using these parameter values, which are determined by reference to the following studies: a) Bowie et al. 1985; b) Reynolds et al. 1987; c) Brookes and Ganf 2001; d) Long et al. 2001; e) Yoshiyama and Nakajima 2002; f) Huisman et al. 2004; g) Sigee 2005; h) Huisman et al. 2006; i) assigned in this study. The references for the absorption coefficient by cyanobacteria in f) and the maximum growth rate of cyanobacteria in c) and g) are for *Microcystis*. The references for light intensity and the maximum growth rate are regarded as averaged values.

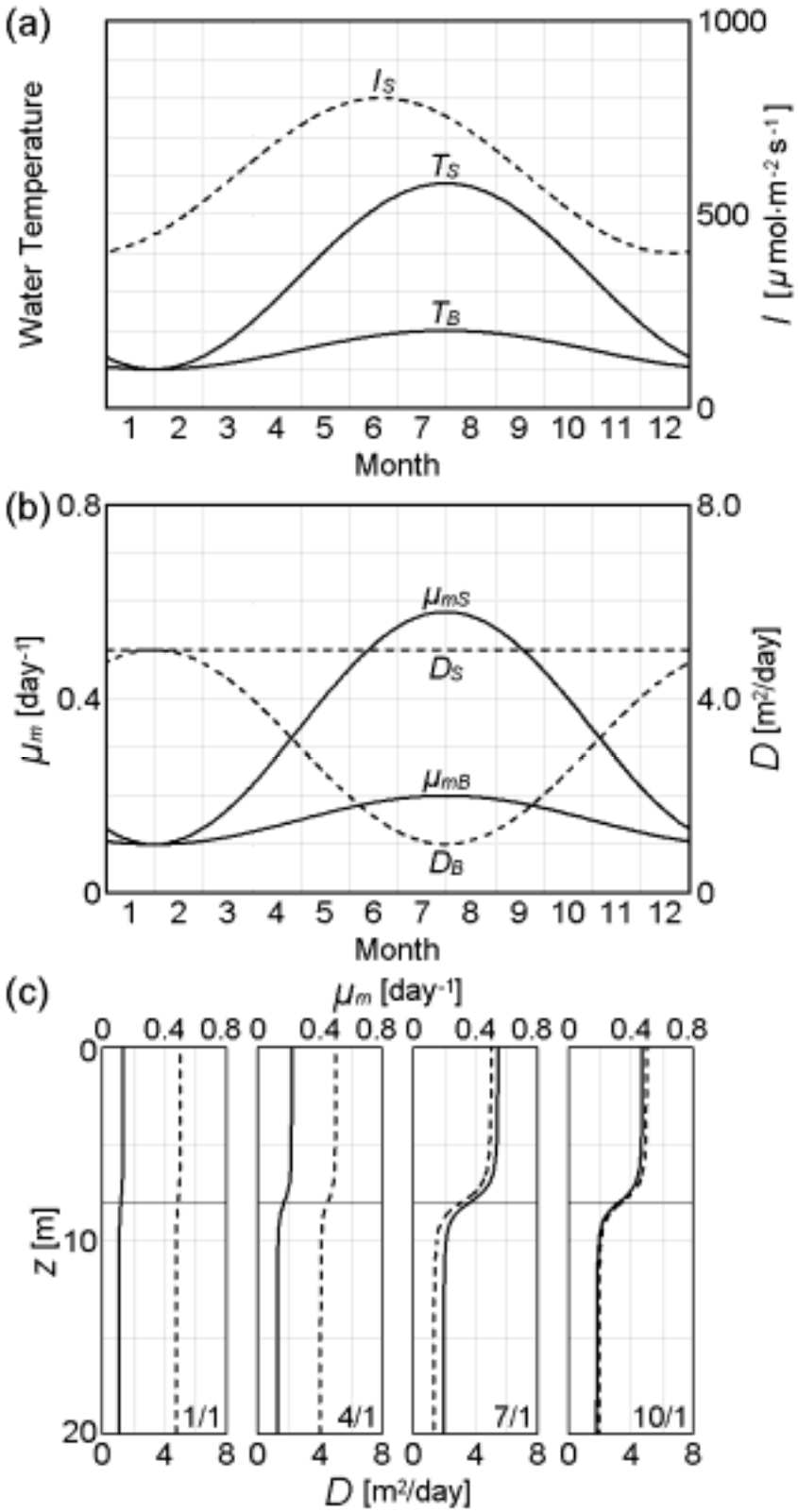

Fig. 1. (**a**) Annual variations of water temperature at the surface (solid line: T_S) and at the bottom (solid line: T_B), and light intensity at the surface (broken line: I_S). The unit of water temperature is arbitrary. (**b**) Annual variations of maximum growth rate of cyanobacteria at the surface (solid line: μ_{mS}) and at the bottom (solid line: μ_{mB}), and turbulent diffusivity at the surface (broken line: D_S) and at the bottom (broken line: D_B). (**c**) Annual variations of vertical distributions of maximum growth rate (solid lines) and turbulent diffusivity (broken lines) in four seasons. The horizontal lines at z=8 m indicate the depth of the thermocline.

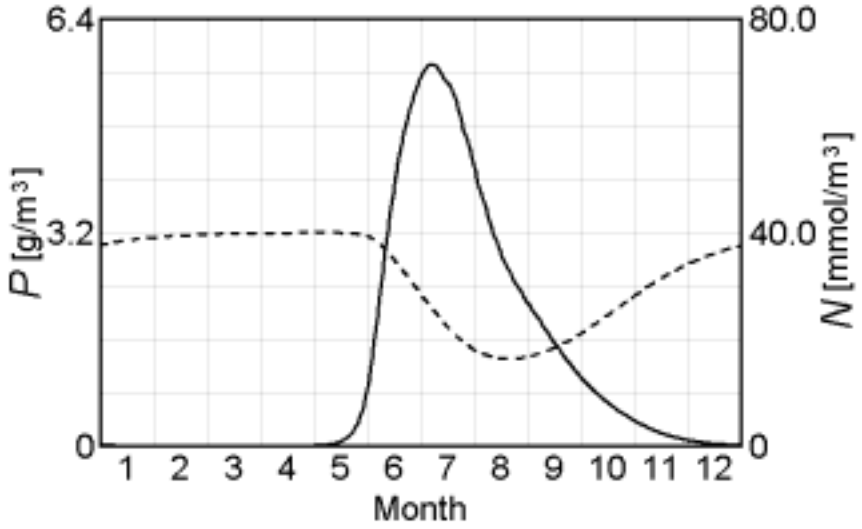

Fig. 2. Annual variations of nutrient concentration (broken line) and cyanobacteria biomass (solid line). Both values are diurnally averaged and also vertically averaged in layers between 0 and 2 m depth.

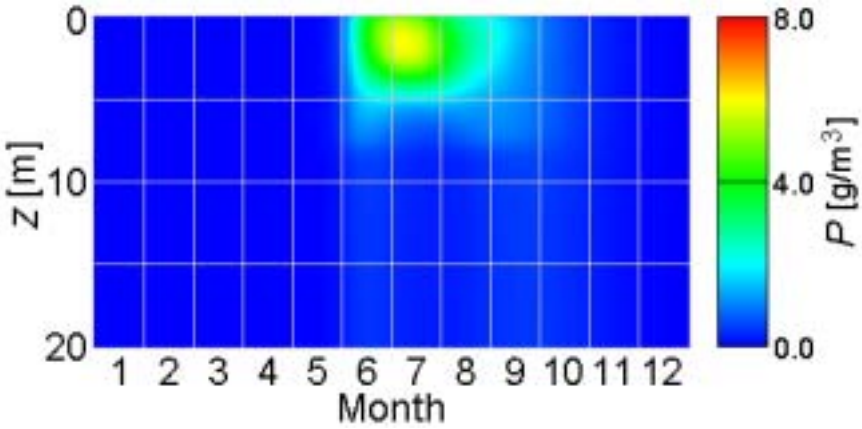

Fig. 3. Annual variation of the depth profile of cyanobacteria biomass. A year consists of 365 days.

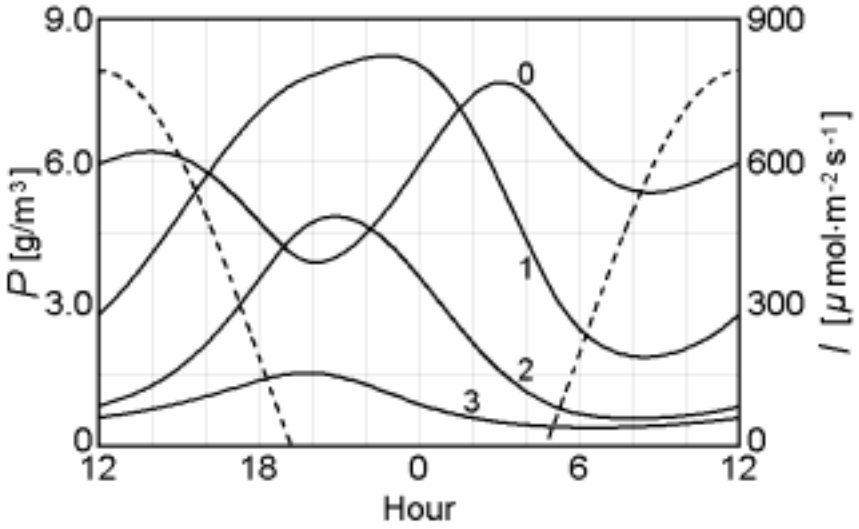

Fig. 4. Diurnal variations of light intensity (broken lines) and cyanobacteria biomass (solid lines) from noon July 10 to noon July 11. The value of *P* is vertically averaged in layers between 0 and 2 m (**0**), 2 and 4 m (**1**), 4 and 6 m (**2**), and 6 and 8 m (**3**) depth.

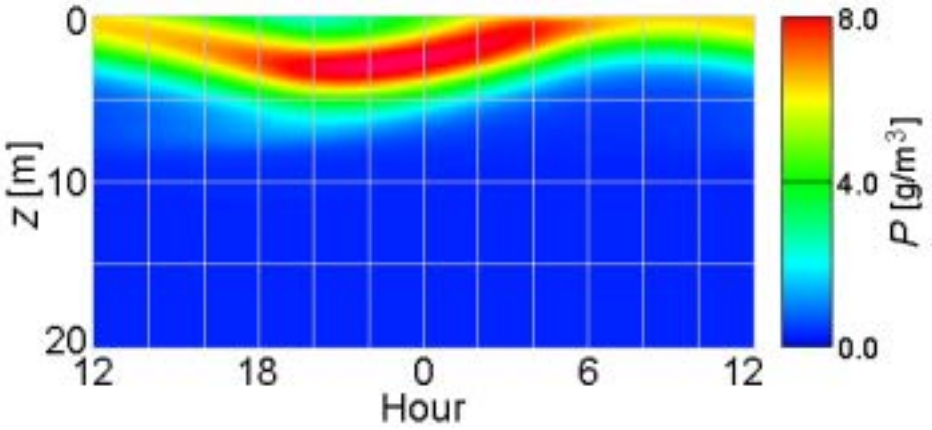

Fig. 5. Diurnal variation of the depth profile of cyanobacteria biomass from noon July 10 to noon July 11.

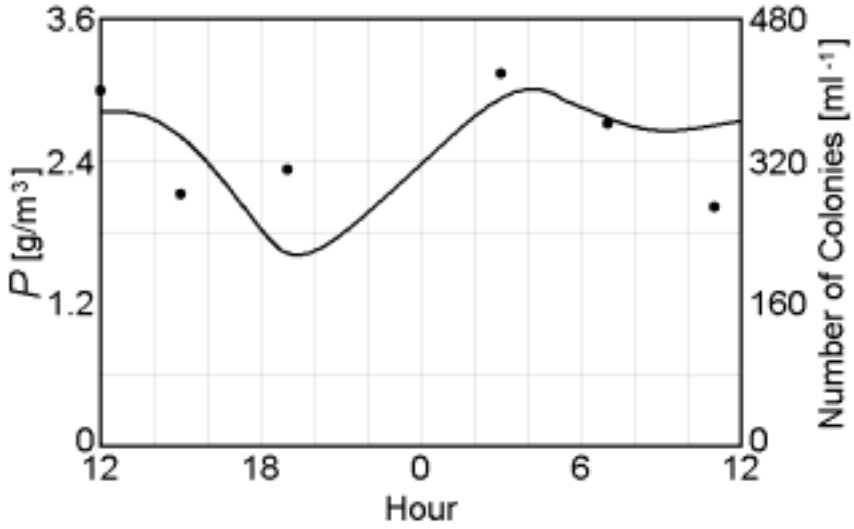

Fig. 6. Comparison between field data (●) and the computer simulation (solid line) for diurnal variation of cyanobacteria biomass. The number of *Microcystis* colonies (●) is the average of two samples taken at 0 and 1 m below the surface in Lake Vinkeveen, the Netherlands, on August 23-24, 1989 (Ibelings et al. 1991). The solid line shows the simulation result of diurnal variation of cyanobacteria biomass from noon August 23 to noon August 24. The value of P is vertically averaged in layers between 0 and 1 m depth. A peak of colony number observed in the early morning is properly simulated in our model.

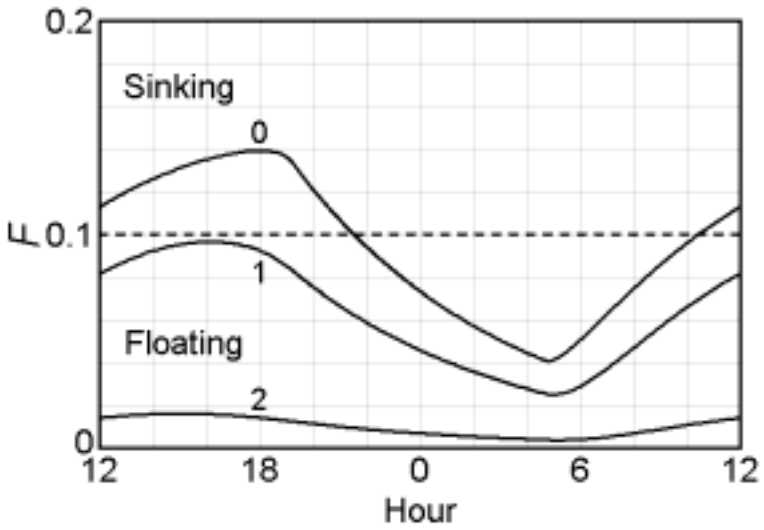

Fig. 7. Diurnal variation of the ballast factor (solid lines) from noon July 10 to noon July 11. The value of F is vertically averaged in layers between 0 and 4 m (**0**), 4 and 8 m (**1**), and 8 and 20 m (**2**) depth. The ballast factor for neutral buoyancy F_0=0.1 is also indicated (broken line).